189. Complexes of the Triolide from (*R*)-3-Hydroxybutanoic Acid with Sodium, Potassium, and Barium Salts: Crystal Structures, Ester Chelates and Ester Crowns, Crystal Packing, Bonding, and Electron-Localization Functions

by **Dieter Seebach***, **H. Michael Bürger**[1]), and **Dietmer A. Plattner**[1])

Laboratorium für Organische Chemie, Eidgenössische Technische Hochschule, ETH-Zentrum, Universitätstrasse 16, CH–8092 Zürich

and **Reinhard Nesper*** and **Thomas Fässler**

Laboratorium für Anorganische Chemie der Eidgenössischen Technischen Hochschule, ETH-Zentrum, Universitätstrasse 6, CH–8092 Zürich

(28.VII.93)

The triolide of (*R*)-3-hydroxybutanoic acid ((*R*,*R*,*R*)-3,7,11-trimethyl-2,6,10-trioxadodecane-1,5,9-trione; **1**), readily available from the corresponding biopolymer P(3-HB) in one step, forms crystalline complexes with alkali and alkaline earth salts. The X-ray crystal structures of three such complexes, (3 NaSCN)·4 **1** (**2**), (2 KSCN)·2 **1**·H_2O (**3**), and (2 $Ba(SCN)_2$)·2 **1**·2 H_2O·THF (**4**), have been determined and are compared. The triolide is found in these structures *i*) as a free molecule, making no contacts with a cation (clathrate-type inclusion), *ii*) as a monodentate ligand coordinated to a single ion with one carbonyl O-atom only, *iii*) as a chelator, forming an eight-membered ring, with two carbonyl O-atoms attached to the same ion, *iv*) as a linker, using two carbonyl O-atoms to bind to the two metals of an ion-X-ion unit (ten-membered ring), and *v*), in a crown-ester complex, in which an ion is sitting on the three unidirectional C=O groups of a triolide molecule (*Figs. 1–3*). The crystal packing is such that there are columns along certain axes in the centers of which the cations are surrounded by counterions and triolide molecules, with the non-polar parts of **1** on the outside (*Fig. 4*). In the complexes **2–4**, the triolide assumes conformations which are slightly distorted, with the carbonyl O-atoms moved closer together, as compared to the 'free' triolide **1** (*Fig. 5*). These observed features are compatible with the view that oligo (3-HB) may be involved in the formation of Ca polyphosphate ion channels through cell membranes. A comparison is also made between the triolide structure in **1–4** and in enterobactin, a *super* Fe chelator (*Fig. 5*). To better understand the binding between the Na ion and the triolide carbonyl O-atoms in the crown-ester complex, we have applied electron-localization function (ELF) calculations with the data set of structure **2**, and we have produced ELF representations of ethane, ethene, and methyl acetate (*Figs. 6–9*). It turns out that this theoretical method leads to electron-localization patterns which are in astounding agreement with qualitative bonding models of organic chemists, such as the 'double bond character of the CO–OR single bond' or the 'hyperconjugative $n \rightarrow \sigma^*$ interactions between lone pairs on the O-atoms and neighbouring σ-bonds' in ester groups (*Fig. 8*). The noncovalent, dipole/pole-type character of bonding between Na^+ and the triolide carbonyl O-atoms in the crown-ester complex (the Na–O=C plane is roughly perpendicular to the O–C=O plane) is confirmed by the ELF calculation; other bonding features such as the C≡N bond in the NaSCN complex **2** are also included in the discussion (*Fig. 9*).

Introduction. – We have recently reported that the cyclic trimer **1** of (*R*)-3-hydroxybutanoic acid is readily available by direct degradation of the biopolymer poly((*R*)-3-hydroxy-butanoate) (P(3-HB)) under acid-catalyzed conditions (thermodynamic control) [1] [2]. As indicated by the formula **1**, the three C=O groups of this triolide point into the same direction, in a conformation which was found in the crystal structure [2], and which

[1]) Part of the Ph. D. thesis work of *H. M. B.* and of *D. A. P.* (Dissertation No. 10283) ETH-Zürich, 1993.

is also present in solution, as deduced from a detailed analysis of the NMR spectra and from the large dipole moment of **1** (4.6 Debye in CCl_4 [2]; 1.72 Debye for MeCOOMe [3]). Since linear oligo(3-HB) containing between 100 and 200 HB units has been postulated to be involved in complexing calcium polyphosphate as part of an ion channel through cell membranes (see the review article [4], and [5]), we thought that the triolide with its three unidirectional C=O groups could serve as a model for the complexation of ions by oligo(3-HB) derivatives. In fact, ion-transport experiments which we have performed in a parallel investigation [6] proved that the (*R,R,R*)-triolide **1** is a more efficient ionophor than its (*R,R,S*)-isomer (with only two unidirectional C=O groups). Also ^{1}H-NMR analysis of CD_3OD solutions containing alkali iodides and the triolide **1** or the analogous tetrolide showed some changes of the coupling constants, indicating minor conformational changes, with the former, but not with the latter oligolide [7].

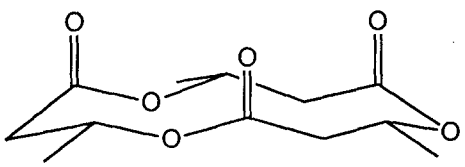

1

2 Na complex: (3 NaSCN)·4 **1**

3 K complex: (2 KSCN)·2 **1**·H_2O

4 Ba complex: (2 $Ba(SCN)_2$)·2 **1**·2 H_2O·THF

Crystallization and X-Ray Crystal Structure Analyses. – Crystallization experiments with the triolide **1** and various alkali salts led to the following conclusions: *i*) with K, use of the thiocyanate counterion [8] leads to crystallizations more readily than with the halides, cyanide, or tetraphenyl borate; *ii*) protic solvents are not as good as are THF, MeCN, $MeCO_2Et$, probably because the complexes of the salts with the triolide **1** are weaker than is their solvation by OH-containing solvents.

Thus, from a solution of NaSCN in MeCN, containing a stoichiometric amount or a slight excess of triolide **1**, crystals suitable for X-ray diffraction were obtained. The composition was (3 NaSCN·4 **1**) (**2**). The coordinates of this structure have been already published [1] and submitted to the *Cambridge Structural Data Base*. A look at a larger section of the structure of **2** (*Fig. 1, a*) reminds of the chaos in a solution! Closer inspection reveals that there are four types of triolide molecules in this structure: *i*) those making no contact at all with Na^+; *ii*) those using a C=O O-atom for a single contact with Na^+ and another one for a bridging C=O(Na^+)$_2$ between two Na^+ ions; *iii*) those forming a chelate C=O–Na–O=C and at the same time bridges between Na^+ ions with their C=O O-atoms; *iv*) finally, there are triolides forming the crown-ester complex, using all three of their C=O O-atoms for contact with the same Na^+ (*Fig. 1, b* and *c*), and simultaneously two of their C=O O-atoms act as bridging elements. This series of different coordinating situations can be thought of as if a single Na^+ ion is moving through a triolide structure. All Na^+ ions are hexacoordinate bearing 5 to 3 C=O

O-atoms and, accordingly, 1 to 3 thiocyanate N-atoms as ligands (*Fig. 1, d*). All SCN^- ions are bridging between two Na^+ ions, so that four-membered rings[2]) (Na–N–Na–N and Na–N–Na–O) result (see caption of *Fig. 1*). While there are numerous crystal structures of crown-ether complexes with ions, as well as complexes containing ester carbonyl *and* ether oxygen ligands, or amide oxygens around the metal [10], the ester crown seen in the present structure is unique.

The isolation of single crystals of a K complex with triolide **1** was somewhat tricky, until we realized that a certain amount of H_2O is required for suitable crystals to form. The complex **3** which eventually was subjected to X-ray analysis contained, in addition to KSCN and triolide **1**, one H_2O molecule in the asymmetric unit (ratio 2:2:1, see *Fig. 2, a* and *b*, for a larger and smaller section of the crystal structure). There is no crown-ester substructure, all triolides form contacts with K which is octahedrally hexacoordinate. There are again chelates between a triolide molecule and K, and four-membered rings containing O–K–O–K[2]).

The only alkaline-earth-ion complex we could isolate in well grown single crystals is **3**. The crystals separating from THF solvent contained, in addition to $Ba(SCN)_2$ and the triolide **1**, H_2O and THF molecules (ratio 2:2:2:1). Salts of the biologically relevant ions Mg^{2+} and Ca^{2+} have so far not formed single crystals containing triolide **1**, in our hands. The structure of complex **3** is shown in *Fig. 3, a* and *b*. The two different Ba^{2+} ions present are nonacoordinated. One of the H_2O molecules is bridging two Ba^{2+} ions. Otherwise there are great similarities of **4** with the Na and K complexes **2** and **3** (four-membered rings, bicyclic arrangements, chelates, but no crown).

In connection with the possible role PHB may play in the formation of ion channels [5], it was interesting to have a look at the crystal-packing patterns of the triolide **1** and of the complexes **2–4** (see *Fig. 4*). The triolide molecules are stacked along the axis of their dipol moment, with opposite direction in adjacent layers[3]) (see *Fig. 4, a*). A view along the crystal axis to which the Na-ions of complex **2** are aligned parallel (*Fig. 4, b*) reveals that the complexed triolides are assembled around the Na-ions in a columnar structure (Na/**1** 1:1), while an additional triolide molecule occupies space in between the columns, *being like a host in a clathrate*. One recognizes a stack of triolide molecules complexing with all three C=O O-atoms and two stacks with only two (one of the stacks with chelating triolide **1**). In the complex **3** containing K and triolide in a 1:1 ratio, there is again a crystal axis with parallel column-like arrangements of KSCN and triolide molecules (only two different types of positions, *Fig. 4, c*). Finally, in the Ba complex **4**, as seen in *Fig. 4, d*, the THF molecules coordinate to the metal in such a way that their planes are arranged perpendicular to the axes around which the divalent cations are grouped. The packing pattern in all three compounds is in agreement with the assumption that properly arranged C=O groups of oligo(3-HB) may provide complexation for ions in a lipophilic environment.

The geometry of the triolide with three approximately parallel C=O groups is preserved in the complexes; superpositions of the free triolide **1** with the triolides complexed to the ions reveals, however, that the C=O O-atoms can move somewhat together for

---

[2]) For review articles containing the structures of similar four-membered rings with alkali atoms, arranged as single units, as cubes, as hexagonal prisms, as ladders, *etc.* see [9].

[3]) This means that **1** is not a candidate for nonlinear optics applications.

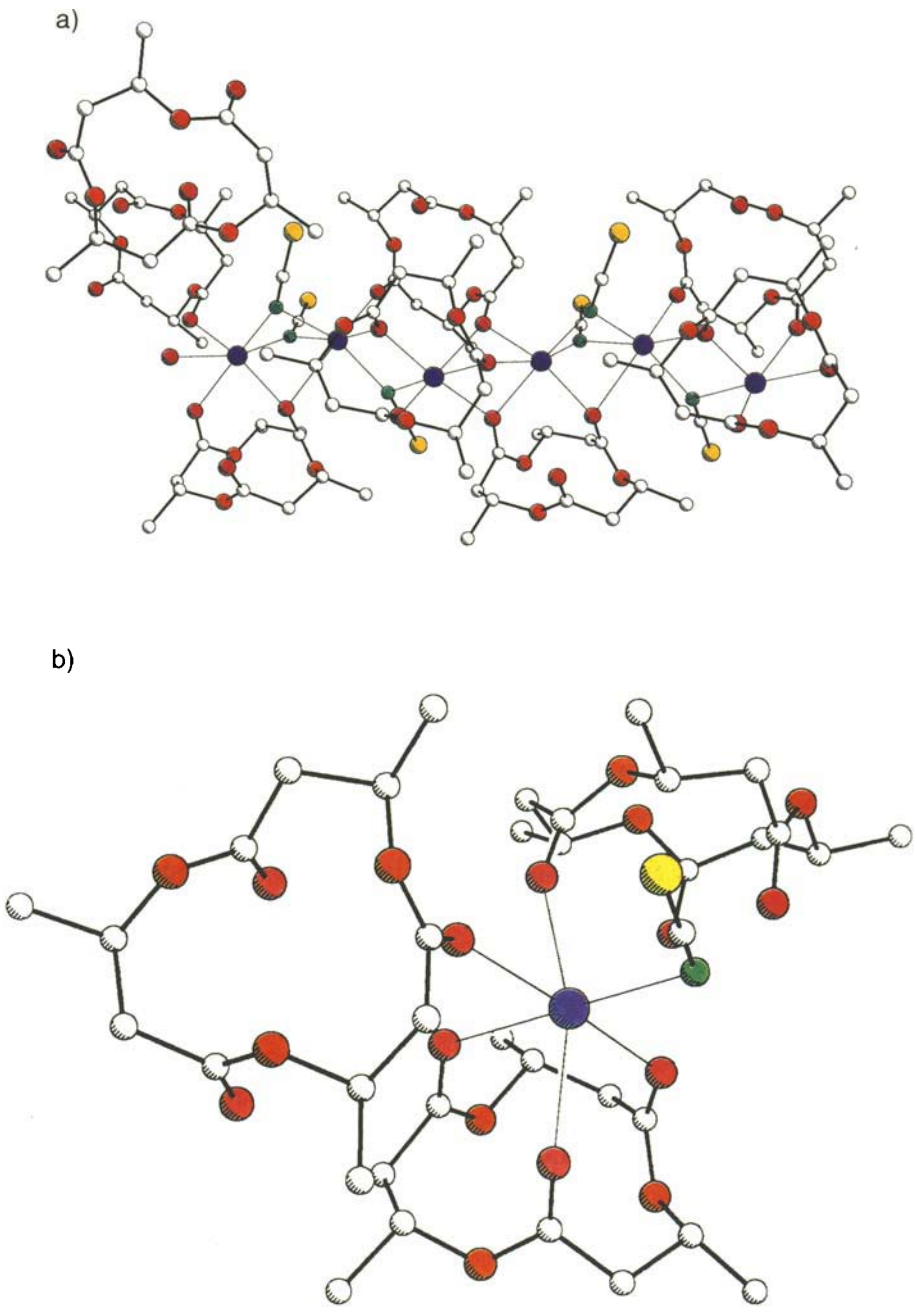

Fig. 1. *Crystal structure of the NaSCN triolide complex* **2**. *a*) A representative section of the structure containing the four different types of triolides making zero, one, two (chelate), and three (crown) contacts with Na^+ ions; a helical arrangement of the Na^+ ions can be recognized; thiocyanate N-atom and C=O O-atom act as bridges between the cations, forming four-membered rings (Na–N–Na–N, Na–N–Na–O, Na–O–Na–O) and bicyclo[1.1.1]

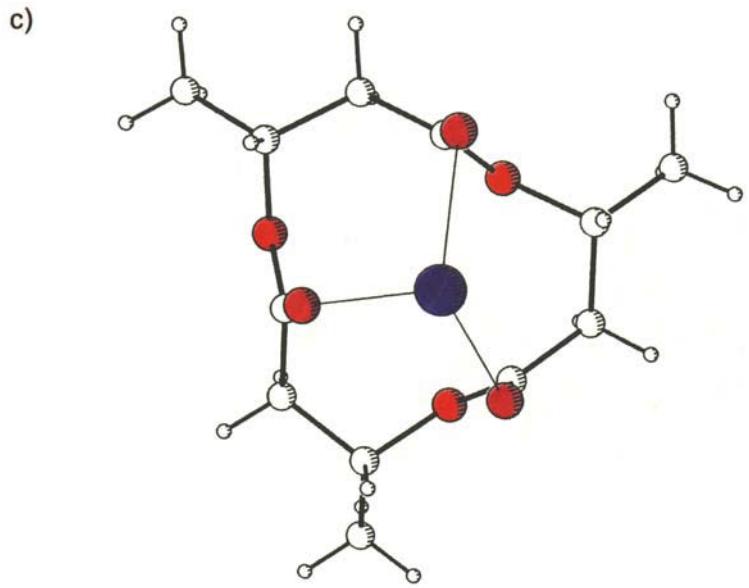

arrangements (in the organic chemist's nomenclature). In the representation of this structure, as shown in [1], a carbonyl O-atom on one of the triolides was missing; also, a different perspective was chosen for **2** here, in order to facilitate comparison with the structures of **3** and **4** (*Figs. 2* and *3*). *b*) Section of the structure of **2** containing the ester crown in which the Na occupies a position near the negative ends of the C=O dipols (dipole moment of the triolide: 4.6 Debye [2]). *c*) View along the pseudo C_3 axis of the Na-crown structural unit. *d*) Complete coordination sphere of the three different Na^+ ions in **2**, with C=O O-atoms red and thiocyanate N-atoms green; on the left side is the Na^+ ion which is part of the crown-ester complex; the Na^+ ion in the middle is chelated by two C=O O-atoms of a triolide molecule; the three C=O O-atoms around the Na^+ ion on the right belong to three different triolide molecules. The arrangements around the Na are in between distorted trigonal prisms and distorted octahedra.

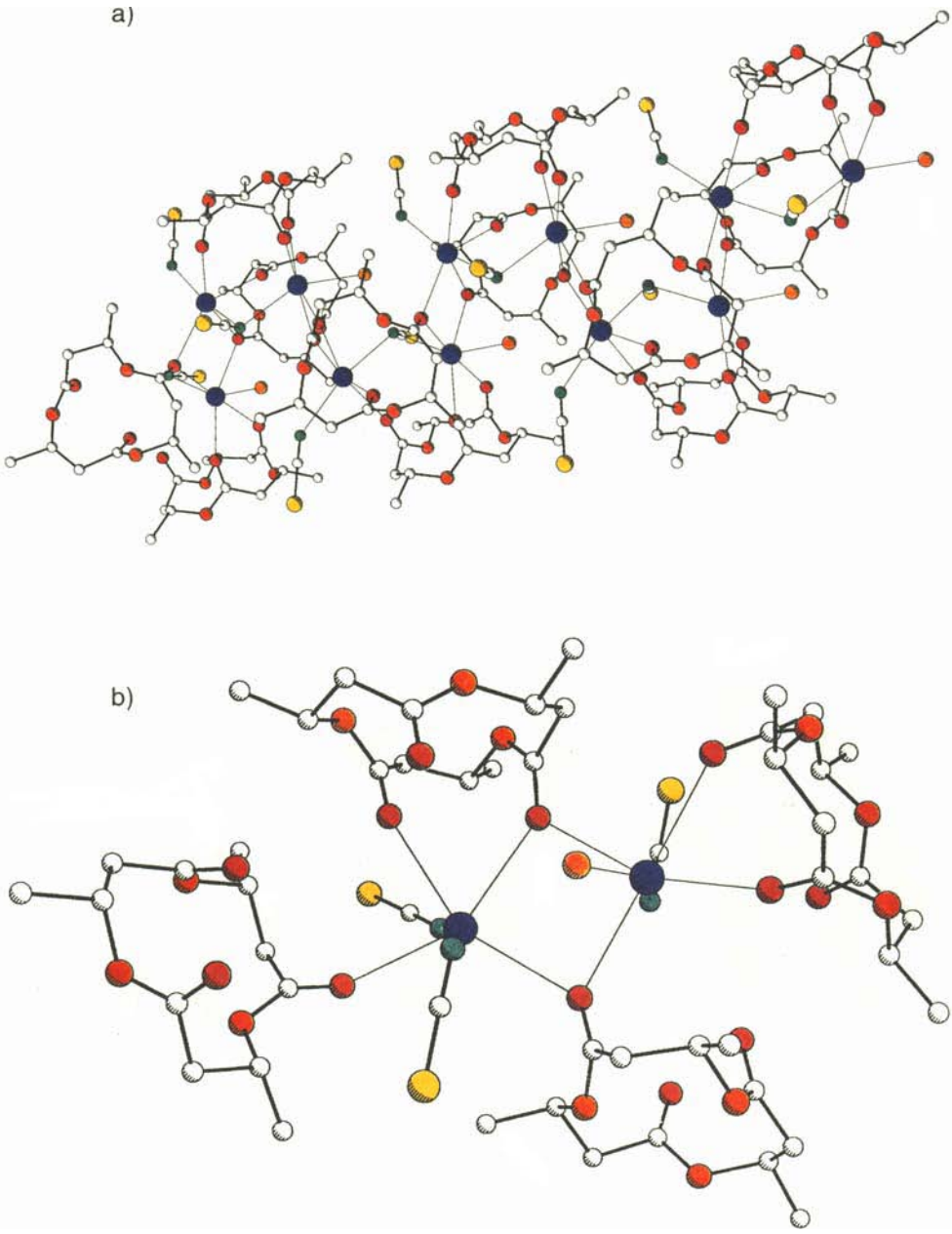

Fig. 2. *Crystal structure of the K complex* **3**. *a*) Section of the structure showing all varieties of complexation between K^+ cations and triolide molecules or thiocyanate anions. *b*) Detail of the structure **3** with two chelating triolides, one of them at the same time chelating with a K^+ and bridging between two K^+ ions. One of the K^+ ions K(1) has a H_2O molecule as ligand.

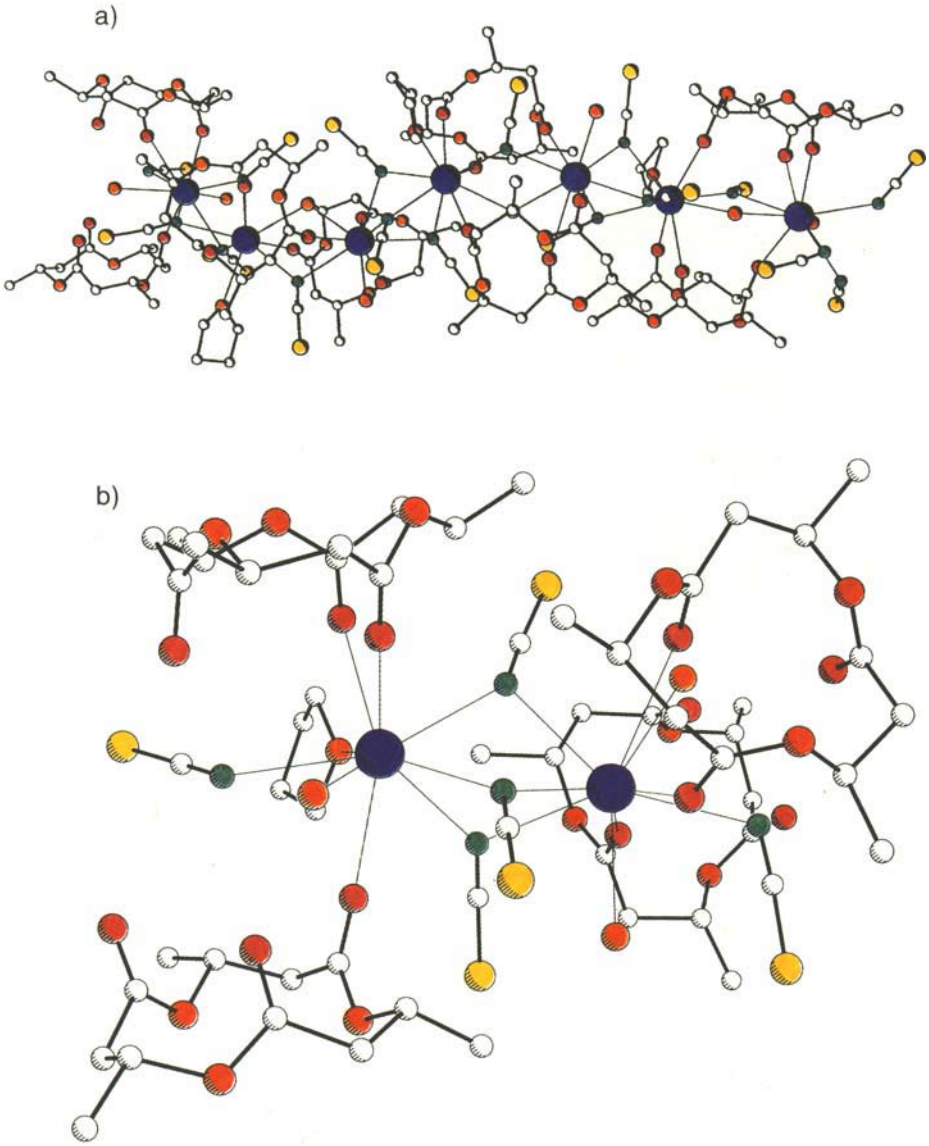

Fig. 3. *Crystal structure of the Ba complex* **4**. *a*) PLUTO plot of a section of **4** containing all characteristic structural features of the complex. The coordination sphere of Ba is crowded by 9 ligands, containing triolide C=O, THF, and water O-atoms, as well as SCN^- N-atoms. There is one C=O O-atom at a somewhat larger distance of 3.26 Å, as compared to the mean value 2.76(11) Å of the other five C=O···Ba distances in the structure. We recognize two types of neighborhoods between Ba^{2+} ions. In one, there is a bridge by three N-atoms of SCN^-, in the other one, there are an SCN^- and a H_2O molecule as well as two triolides bridging; these triolides act like clamps to form ten-membered rings of –Ba–N–Ba–O=C–O–C–C–C=O–. The O-atom of THF is not involved in bridging between Ba^{2+} ions. *b*) Section of **4** with the tricyclic arrangement of three four-membered –Ba–N–Ba–N– rings containing the SCN^- counterions. The structure of **4** was determined by *Paul Seiler* of the X-ray crystallographic service division, Laboratorium für Organische Chemie, ETH-Zürich.

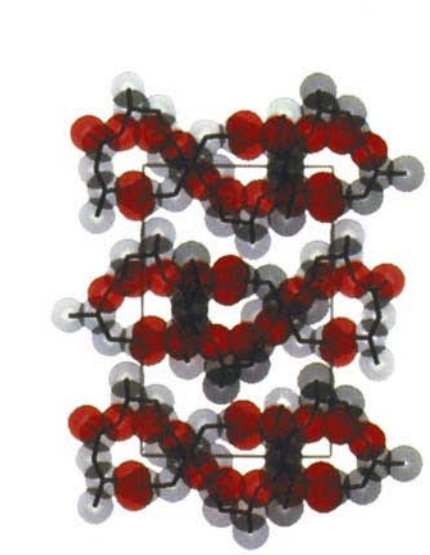

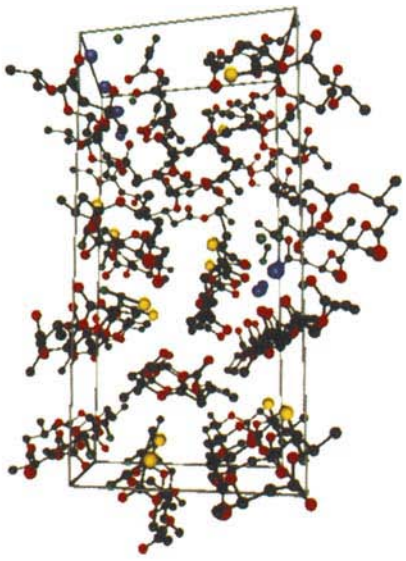

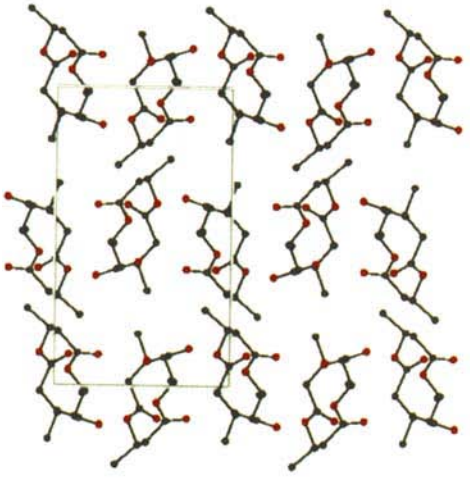

a)

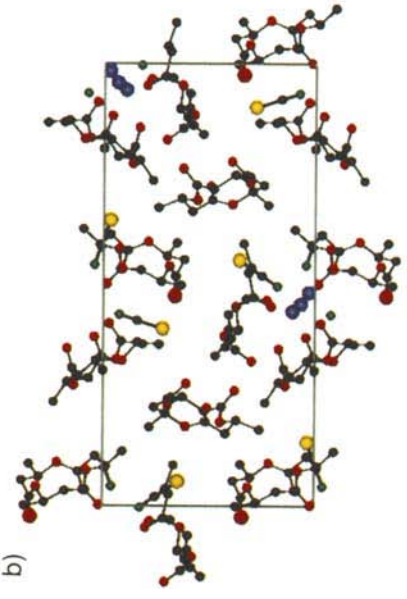

b)

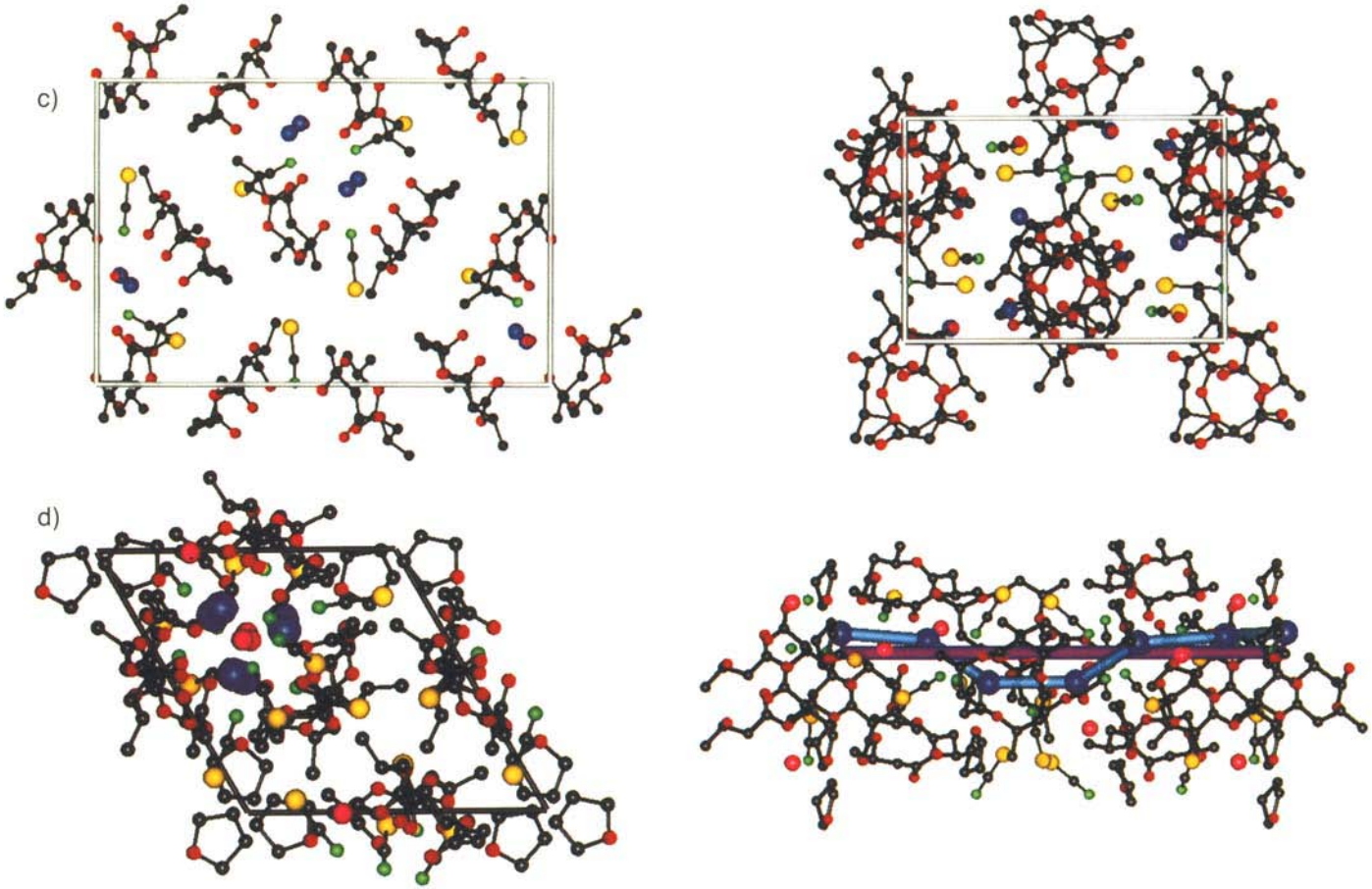

Fig. 4. *Three-dimensional representations of the packing in the crystal structures of the triolide* **1** *and of the complexes* **2**, **3**, *and* **4** (cations: blue, C: black, O: red, N: green, S: yellow, H_2O: light blue, [10]): *a*) Triolide **1** (*left*: parallel projection along [010], *right*: along [100]); the structure has been published in [1] [2]. *b*) Na Complex **2** (*left*: parallel projection along [100], *right*: skew perspective projection close to [100]). *c*) K Complex **3** (*left*: parallel projection along [100], *right*: along [001]). *d*) Ba Complex **4** (*left*: parallel projection along [001]); the structure contains three helical arrangements centered around [00*z*], [2/3 1/3, *z*], and [1/3 2/3, *z*] (*right*: helical arrangement around the H_2O-Ba channel in the structure of **4**, centered by the purple rod which encloses the H_2O molecules; the helix of Ba^{2+} ions is nicely visible and emphasized by blue connections).

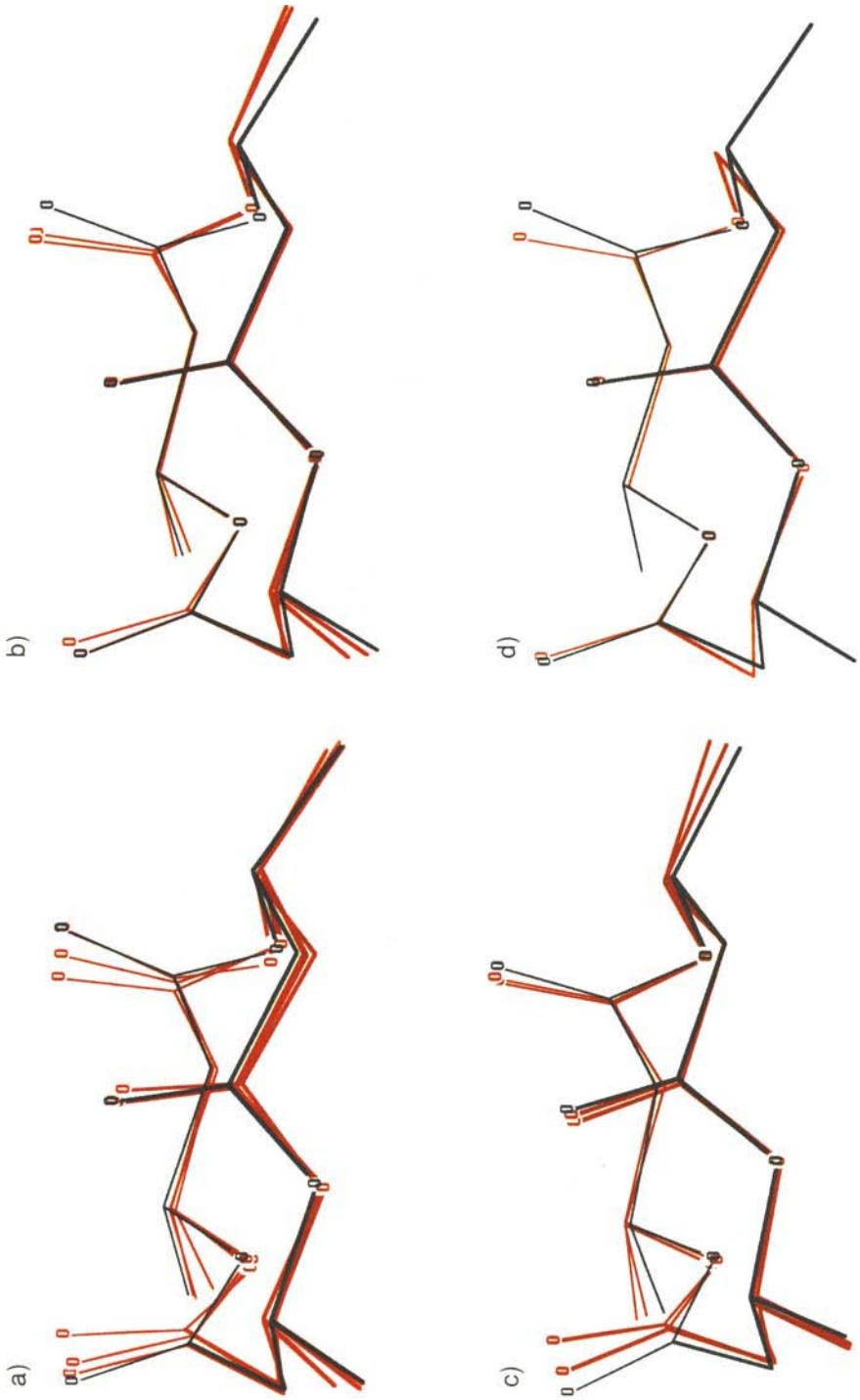
b)
d)
a)
c)

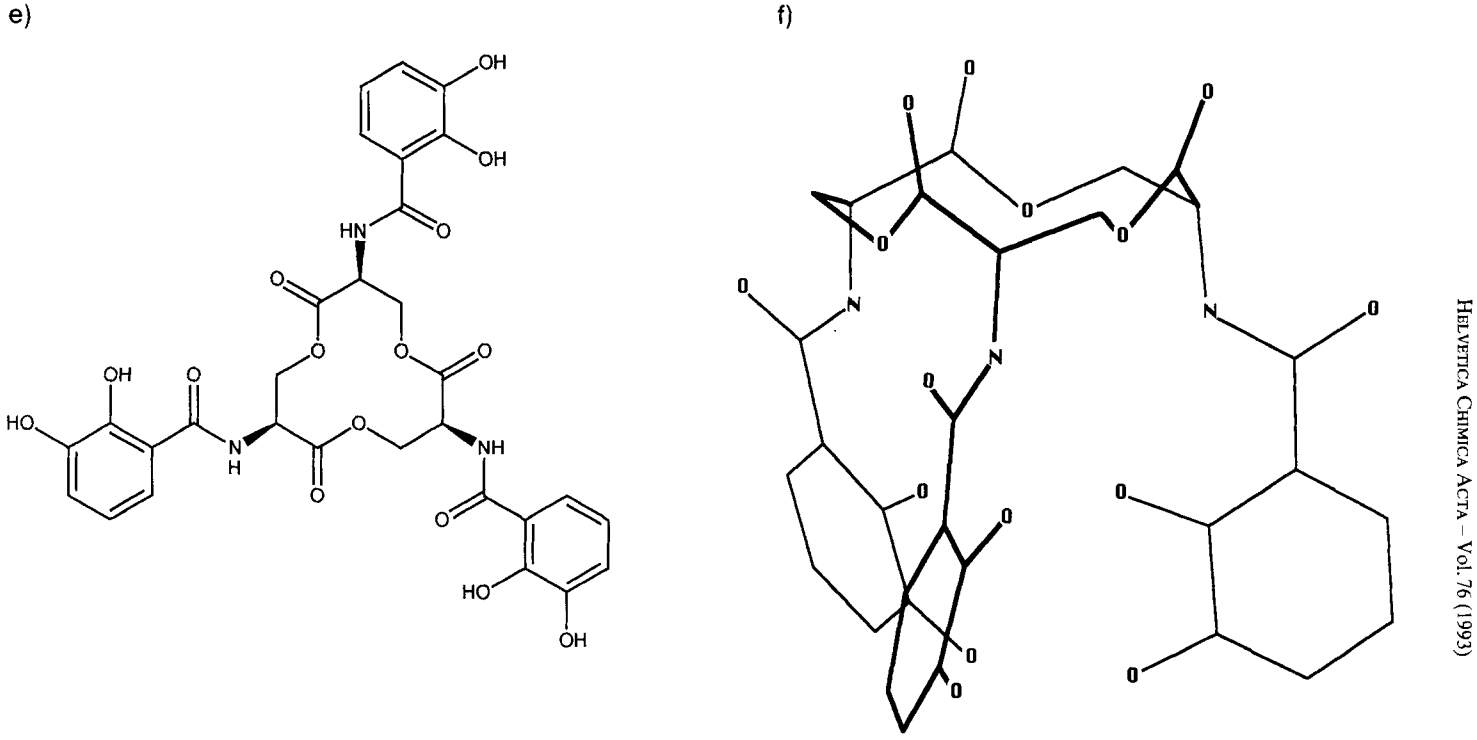

Fig. 5. *Superposition of the triolide molecules as present in the crystal structures of the free ligand* **1**, *of the complexes* **2**–**4**, *and of Enterobactin.* The free triolide **1** [2] is drawn in black, the triolides from the other structures in red. The structural presentations in this figure were generated from the crystal coordinates and presented using the MacMoMo program by *Max Dobler* (Laboratorium für Organische Chemie, ETH-Zürich). *a*) Ligand **1** and the three complexing different triolides in **2**. *b*) Ligand **1** and the two different triolides in the K complex **3**. *c*) Ligand **1** and the two different triolides in the Ba complex **4**. *d*) Ligand **1** and the triolide unit in enterobactin [11a]. *e*) Formula of enterobactin, a serine-derived triolide with 2,3-dihydroxybenzoyl groups on the N-atoms; enterobactin is a Fe chelator with a binding constant of *ca.* 10^{50} [11b]. *f*) Section containing the enterobactin moiety in a V complex [11a]; V^{IV}, other cations, and their ligands have been omitted from the crystal structure for clarity.

better chelation (see *Fig. 5*). A comparison of our triolide **1** with the analogous structural segment of the enterobactin V^{IV} complex [11] is also shown in *Fig. 5*. In the *Table*, we have collected the angles and distances which describe the geometries of complexation of the ions to the C=O groups occurring in the three complexes[4]). In no case is the ion located exactly in the C=O plane, with a mean deviation angle α from planarity of 26.9° and a maximum of 61°. Also, the projections of the ions (M) onto the C=O planes generate C=O–M angles β averaging to 156° over all structures (see the *Table*).

Table. *Geometries of Complexation of the Metal Ions Na^+, K^+, and Ba^{2+} with the Triolide C=O Groups in* **2–4**. The angles α and β are defined as indicated in the accompanying presentation (*cf.* also [13a, c]). The positions with an asterix mark those C=O groups which are involved in a chelate-type coordination, those with two asterixes belong to the triolides forming the Na ester-crown complex.

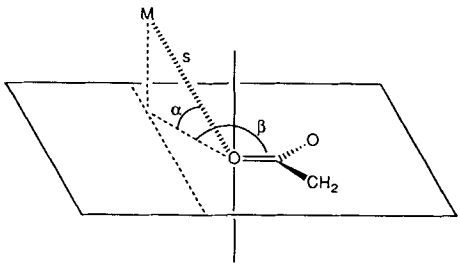

NaSCN Complex **2**			KSCN Complex **3**			$Ba(SCN)_2$ Complex **4**		
α [°]	β [°]	s [Å]	α [°]	β [°]	s [Å]	α [°]	β [°]	s [Å]
32.9	179	2.49**	7.0	162	2.71*	2.0	159	3.26*
51.6	154	2.50**	41.1	168	2.80*	38.7	172	2.72*
49.8	170	2.42**	29.4	153	2.86*	32.3	170	2.76*
35.1	147	2.50*	4.9	145	2.80*	6.9	165	2.94*
16.7	141	2.36*	9.8	154	2.76	6.1	164	2.71
61.0	144	2.80	24.5	128	2.82	13.3	174	2.66
22.3	143	2.41	27.4	133	2.82			
20.7	156	2.27	41.2	164	3.01			
17.1	159	2.58						
39.5	132	2.44						
29.9	178	2.52						
37.8	161	2.61						

The most interesting structural segment is the novel crown ester present in the Na complex **2**. As can be seen from *Fig. 1, c*, and from the *Table*, the planes containing Na–O=C and the C=O planes form angles of 154, 170, and 179°. In our preliminary publication [1], we have proposed that the interaction between Na^+ and the three carbonyl O-atoms may best be described as a pole-dipole interaction. If this were true, there should be no electron density which could be associated with bonding electrons between Na and the O-atoms. There is a new computational method by which electron localization [14] can be calculated, and this was applied to complex **2**.

[4]) For a discussion of the geometries in alkali complexes with C=O compounds, see [10] [12] and the review article by *Schreiber* and coworkers [13a]. For complexes of other metals with C=O groups see also [13a] and the recent papers by *Wuest* and coworkers [13b], and *Denmark* and *Almstead* [13c].

Electron-Localization Function (ELF) and Its Interpretation for Ethane, Ethene, Methyl Acetate, and the Complex 2. – We used a quantum-mechanical approach for studying the electron-density and electron-localization characteristics in molecules and solids [14] [15] to analyze the nature of the bonding in organic molecules and extended systems[5]). Chemists have always preferred visual pictures to describe bonding. Localized models, such as the *Lewis* formulae [16], hybrid orbitals [17], and the resonance formalism for conjugated systems [18], are widely and most successfully used [19]. There are many efforts to extract and visualize information from quantum-mechanical calculations, *e.g.* incremental and segmental properties by frontier orbitals [20] or localized orbitals [21] which, however, are not always uniquely defined.

The description of chemical bonding we use here is generated by the so-called electron-localization function (ELF) [14]. It has recently been applied to a variety of systems [15] [22], and has turned out to be a most useful tool yielding three-dimensional representations. Contrary to the electron densities $\rho(x,y,z)$ or difference densities $\Delta\rho(x,y,z)$, ELF(x,y,z) describes chemical bonding in much more detail, leading to distinguished pictures of electron distributions, for instance in σ- and π-bonds or of lone pairs [15]. ELF is a pair correlation function describing the probability P_{12} of finding two electrons of the same spin in a given volume element (*cf.* pair probability in the *Hartree-Fock* treatment [14] or the kinetic-energy distribution in the local-density approximation [22b]). In principle, all occupied electronic states are considered so that P_{12} has the properties of an observable which is invariant to unitary orbital transformations.

Since P_{12} and the localization have an inverse relationship (*Pauli* principle!), a more useful expression is

$$\mathrm{ELF} = \frac{1}{1 + \dfrac{P_{12}}{P_{12}^{EG}}}$$

in which P_{12} is normalized to the probability P_{12}^{EG} in the free-electron gas of the same density. This equation defines the range $0 \leqslant \mathrm{ELF} \leqslant 1$ (highest localization with ELF = 1, electron-gas-type delocalization with ELF = 0.5). In our treatment [15], the densities are color coded (white = high, blue = low localization; see the scale given in *Fig. 6, a*).

For the present study, the molecular orbitals and band structures were calculated by the *Extended Hückel* (EH) method [23] [24]. The ELF calculations were performed with an EH program modified [25] such that two-dimensional and three-dimensional ELF maps (iso-ELF surfaces in space) can be obtained, see *Figs. 6–9*.

To briefly discuss the characteristic features of ELF representations we chose ethane (*Fig. 6*) and ethene (*Fig. 7*).

Fig. 6, a, displays a point pattern of the electron density in which the color is coding for the ELF (see color bar on the bottom of *Fig. 6, a*). The two-dimensional section (two antiperiplanar H- and the C-atoms) shows three pronounced localization areas, one of which is a C,C σ-bond, the other two are the H-atoms. The core regions of the C-atoms show low electron density (*cf.* location of the element symbols), because we are using the EH method which takes into account only the valence electrons[6]). *Fig. 6, b*, is a three-

[5]) We are almost tempted to use the term 'supramolecular systems'.

dimensional sketch of ethane in the staggered conformation with the rotationally symmetric yellow bubble being an iso-ELF surface (ELF = 0.85). This bubble represents the C,C σ-bond.

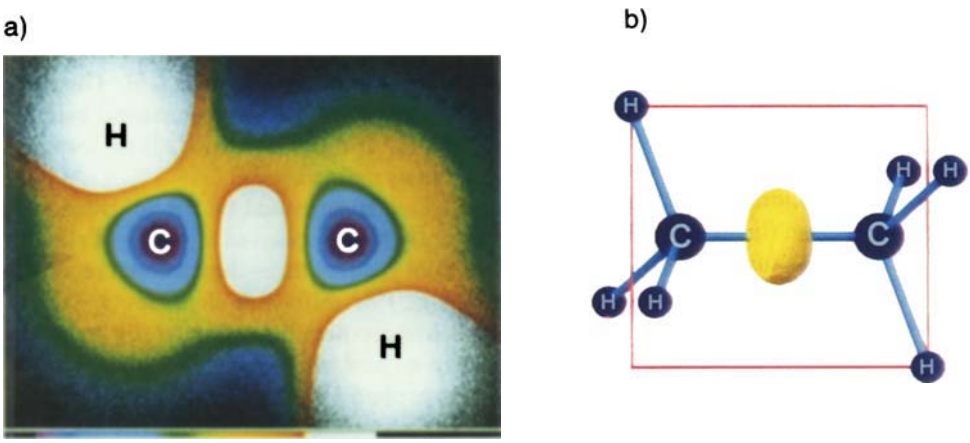

Fig. 6. *ELF Analysis of the ethane molecule. a*) Two-dimensional section through the molecular plane of ethane containing the C–C bond and two of the H-atoms (white patterns). The electron density is represented by the density of points, the color of each single point is a measure of ELF(x,y,z) as given by the color bar at the bottom. The lighter the color the higher the ELF. *b*) Three-dimensional display of an ethane molecule and an iso-ELF surface for the value 0.85 (yellow bubble). The H regimes have been omitted for reasons of clarity.

The corresponding representations for ethene are shown in *Fig. 7*. As can be seen by comparison of *Fig. 6, a*, with *Fig. 7, a* (mean plane section), the σ-bond region of ethene is considerably contracted with respect to that of ethane. A section perpendicular to the molecular plane of ethene is shown in *Fig. 7, b*, with a p-orbital-like localization representing in the σ- and π-bond. The iso-ELF surface of ethene in *Fig. 7, c* is a demonstration of the extension of the regimes[7]), thus shielding attack from directions associated with the molecular plane, but not perpendicular to it. For clarity, we will omit in all following displays the bulky localization spaces around the H-atoms. Finally, the iso-ELF surface of the ethene C=C bond is shown in *Fig. 7, d*, it is remarkable that the ELF treatment leads to a rather small localization space near the inter-atomic vector normally associated with the σ-bond (*cf. Fig. 7, b*).

This characteristic feature of ELF is even more pronounced in triple bonds (N_2, HCCH [15] [27]) and in polar bonds. It should be stressed that the spatial extension of ELF is not a measure of the bond strength. A small ELF volume associated with a high electron density can still be indicative for a strong bond.

---

[6]) In a full-potential, all-electron calculation, the inner shells of the atoms become visible by ELF; the shells are clearly separated from each other, contrary to total-electron-density representations [14].

[7]) The localization areas assigned to the H-atoms are open to the vacuum because ELF = 1 for s^1 and s^2 configurations. Note that spin pairing is not considered in the ELF treatment, and, thus, H and He yield similar distributions.

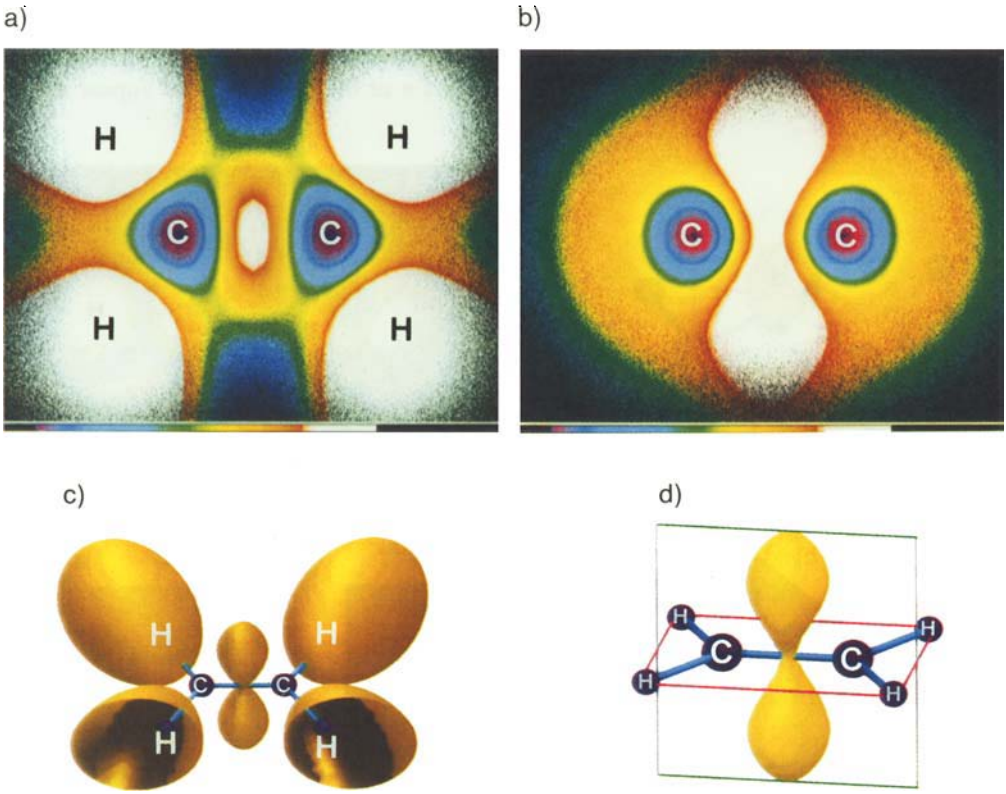

Fig. 7. *ELF Analysis of the ethene molecule. a*) Section of the molecular plane as indicated by the red frame in *d*) showing white regions for the C=C bond and the four H-atoms. *b*) Section perpendicular to the one in *a*) as indicated by the green frame in *d*) with a pronounced elongation of ELF perpendicular to the molecular plane indicating the double-bond character. *c*) Three-dimensional sketch of ethene with iso-ELF surfaces for ELF = 0.85. The large extension of the H regimes is nicely displayed. *d*) As *c*, but ELF is displayed only for the C=C bond region. The characteristic form of the yellow bubble designs the C=C bond.

We are now prepared to analyze the basic chemical unit of our complex **2**, *i.e.* methyl acetate (see *Fig. 8*). For our calculation, we chose the minimum-energy conformation [28][8]). The three-dimensional representation in *Fig. 8, a*, reveals several bonding features with striking resemblance to crude qualitative models used by organic chemists. We see the σ-bond **a** between the C-atoms with a slight deviation from rotational symmetry (a tiny 'π-contribution'). We recognize the C=O bond **b** represented by a p-orbital-type iso-surface much more contracted than in the homopolar C=C bond of ethene. The C–O bond **c** has a π-like deformation compatible with the observed rotational barrier of *ca.* 10 Kcal·mol^{-1} ('double-bond character', resonance structure, *cf. Fig. 8, a, c*, and **A**). The contraction in **c** (C–O) as compared to **a** (C–C), due to the polar-bond character should be noted (cf. *Fig. 8, a* and *8 b*). The so-called nonbonding electron pairs **d** of the CH_3O

[8]) For an analysis of the conformation of esters from 1750 *Cambridge File Structures*, see [29].

oxygen appear as a horse shoe-like localization bubble with pronounced in-plane and out-of-plane components. The latter one is part of the π-interaction (n$\rightarrow\pi^*$ delocalization, see *Fig. 8, e*). The nonbonding electron pairs **e** of the C=O O-atom appear as a

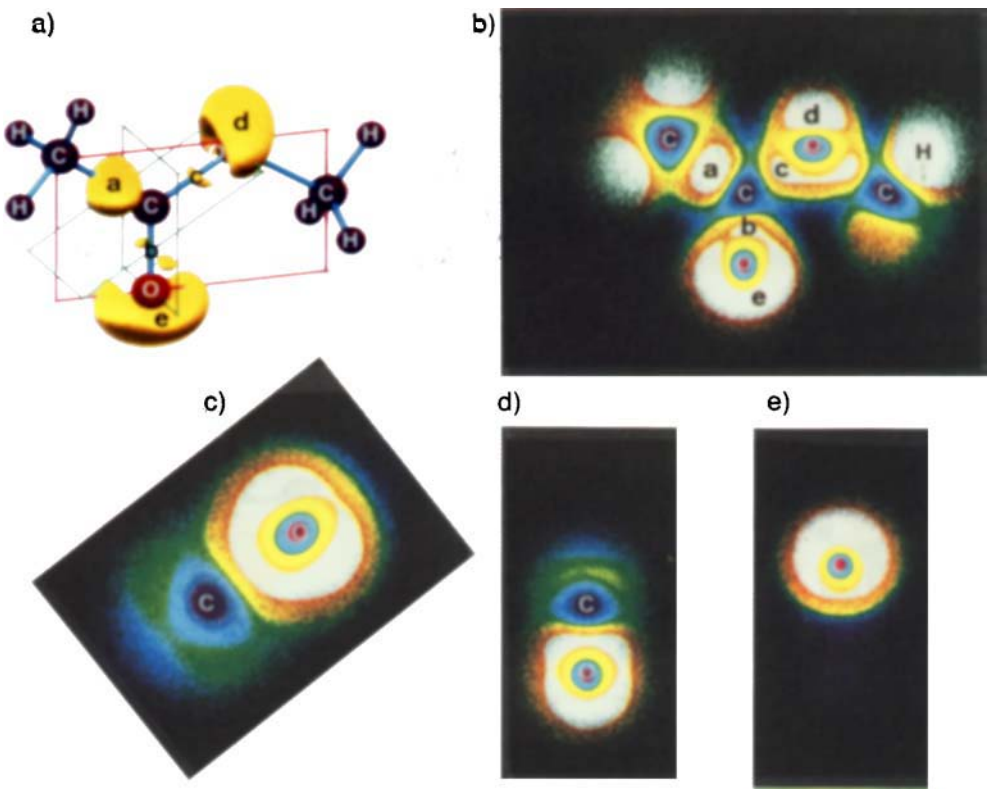

Fig. 8. *ELF Analysis of the methyl acetate molecule. a*) The three-dimensional model with yellow iso-surfaces (ELF = 0.85) shows the spatial regimes of bonding and lone electron pairs. It should be noted that the extension of the latter (in our scheme) reassures beautifully the *Nyholm Gillespie* rules of electron-pair repulsion (VSEPR theory [26]). Contrary to the usual *Lewis* description, there is no separation between the two lone pairs at both, the C=O and the CH_3O O-atoms, respectively. This is true as well for other spatially close localization regions like in the case of σ- and π-bonds, for example. The pronounced contraction of the C,O bond regimes compared to that of the C,C bonds is predicted by the VSEPR theory as well, namely by the rule that electronegative substituents do contract the corresponding bond regimes. *b*) Section through the molecule as indicated by the red frame in *a*. Gross features as well as second-order effects are seen. The small letters **a**–**e** in the picture denote spatial regions which are discussed in the text: **a**, **b**, and **c** mark C–C, C=O, and C–O bond regions, **d** and **e** the C=O and ester O lone pairs, respectively. The distortion of the white C=O lone pair region **e** is in agreement with a n$\rightarrow\sigma^*$ interaction called anomeric effect (*cf.* formula **B**). However, the n$\rightarrow\sigma^*$ donation from CH_3O O-atoms into the carbonyl C,O σ-bond which is also usually considered to contribute to a π-type bonding (see **C**) ist not visible. *c*) A two-dimensional section as shown by the light blue frame in *a*. Comparison of *b* and *c* for the C–O bond region clearly indicates a π contribution as outlined by formula **A**. This is seen in *Fig. 8, a* too. *d*) A cut through the C=O bond **b** as indicated by the green frame in *a*. Comparison of *b* and *d* clearly shows the double-bond character with a strong polarization towards the O-atom. The corresponding yellow bubble in *a* is an iso-value inside the white area of *d*. *e*) Section through the yellow bubble **d** in *a*, parallel to the green frame in *a*. There is no distortion of the lone-pair region **d** compared to the similar lone-pair region **e** in *b*.

banana-shaped localization bubble with its main axis perpendicular to the π-bond (*cf.* *Fig. 8*, *a* and *d*). The form of this bubble is such that there is more localization in a direction anti-periplanar to the CH_3 than to the CH_3O group, in perfect agreement with the view that there is an $n \rightarrow \sigma^*$ interaction also called an anomeric or 'stereoelectronic' effect (*Fig. 8*, *a*, *b*, and **B**) [30]. The detailed two-dimensional ELF dsitribution in *Fig. 8*, *b*, clearly shows the nonsymmetrical localization around the C=O O-atom.

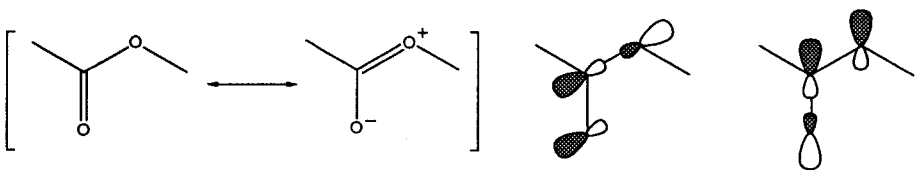

A **B** **C**

The Na complex **2** of the triolide forms a one-dimensional column around a backbone consisting of the Na^+ cations surrounded by the SCN^- counterions and the triolide molecules (see *Fig. 4*, *b*). This *quasi*-one-dimensional structure was analyzed by a one-dimensional band structure calculation of the EH type. Part of this column (corresponding to approximately two unit cells) is shown in *Fig. 9*, *a*, together with iso-ELF bubbles (ELF = 0.85) in the vicinity of one of the Na^+ ions (non-coordinating triolide molecules have been omitted). Each of the three Na^+ ions in the translation period are hexacoordinate by 3–5 C=O O-atoms and 1–3 SCN^- N-atoms. The stereoview in *Fig. 9*, *b*, shows a magnification of the left-hand side of *Fig. 9*, *a*, focussing attention to one of the Na crown-ester components. The high localization spaces (ELF = 0.85, yellow bubbles) around the C=O O-atoms indicate pronounced directionality by their banana shape. It is evident that the long axis of the ELF bubbles is coplanar with the O–C=O group. However, in the chelate and crown-type coordination, these lone-pair regions do not coordinate the Na^+ cations directly. This is indicated by the course of the light-blue Na–O vectors which do not intersect with the ELF bubbles, *i.e.* there is no electron localization between these atoms[9]). For those triolides which coordinate with just one O-atom an ideally directed lone pair bubble is present which is penetrated by the Na–O vector close to the center. There is, however, no deformation of the lone pairs to the Na-atom either, which might indicate a donor function.

A further interesting feature is found at the bridging SCN^- ion: there is a cloud for the N lone pair, as expected, but a torus around the C≡N bond. The latter marks the space of the linear combination of the two π-bonds ($D_{\infty h}$ symmetry), but not that of the C,N σ-bond. This is a common effect in ELF observed for spatial regions with a very high electron population [15] [22]. In summary, we would like to emphasize the following points:

1) The Na^+ cations are electrostatically coordinated by lone pairs of O- and N-atoms which form a cage around the metal.

---

[9]) A charge iteration investigation on Na, N, and O (see computational details), which is sensitive to the effective charge transfer, has been performed with the result of some charge migration from N and O back to Na^+. At the same time, the overlap populations Na–N and Na–O do increase slightly, but the shape of ELF(x,y,z) is unchanged.

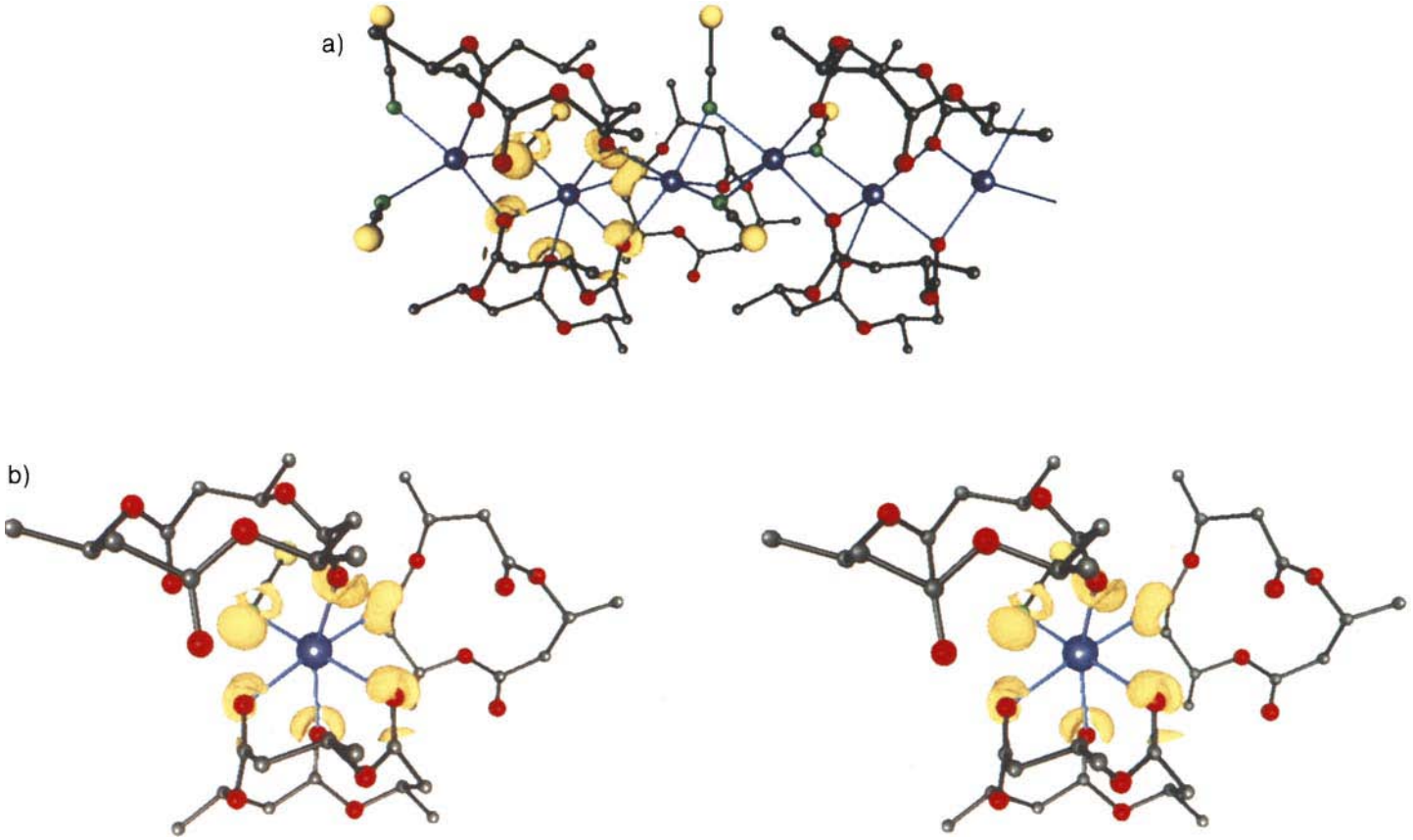

Fig. 9. *ELF Analysis of the NaSCN triolide complex* **2**. *a*) Na Coordination in a NaSCN-triolide chain section corresponding to two unit cells along [100] (Na: large purple spheres, C: black, O: red, N: green, S: yellow). At the left side iso-ELF surfaces (ELF = 0.85) in the vicinity of Na are displayed (yellow bubbles). Six ELF bubbles coordinate the Na in form of a distorted octahedron. The direct connection of Na and four of the C=O O-atoms does practically not interact with the ELF bubbles. Clearly, this type of coordination has an ionic or non-directed character. Hence, there is a geometric difference between the coordination polyhedron of atomic sites and that of electron-localization clouds. *b*) Stereopair of the magnified left part of the structural section shown in *a*.

2) The form of the cage generated by the lone pairs is markedly different from that formed by the corresponding N- and O-atoms. In general, consideration of the arrangement of centers of gravity of the lone pairs around an atom may be more relevant to the understanding of structure and reactivity than the classical description using the atom sites (core positions).

3) ELF(x,y,z) clearly produces features of chemical bonding which can neither be seen from the electron density nor – unambiguously – from hybrid models. We have shown that ELF expresses classical pictures of chemical bonding, such as bond types, lone pairs, diffuseness, deformations, directionality, and second-order effects like hyperconjugation. Since ELF is neither restricted to specific classes of compounds nor to particular types of quantum-mechanical calculations, it can be applied widely on quite different levels of sophistication.

The help of *Florian Kühnle* in preparing the originals for the figures shown in this paper is gratefully acknowledged.

Experimental Part

General. All solvents were of *puriss.* quality. NaSCN was from *Fluka AG* and of *purum* quality, KSCN was also from *Fluka AG*, and *puriss.* $Ba(SCN)_2 \cdot 3H_2O$ was from *Alpha* and 99% pure. M.p.: *Büchi/Tottoli* melting point apparatus, not corrected. IR Spectra (KBr): *Perkin Elmer 983*. Elemental analysis were done by the Microanalytical Laboratory of the ETH-Zürich.

(4R,8R,12R)-4,8,12-Trimethyl-1,5,9-trioxacyclododecane-2,6,10-trione (**1**) was prepared as described in [1].

Tetrakis[(4R,8R,12R)-4,8,12-trimethyl-1,5,9-trioxacyclododecane-2,6,10-trione] Tris(sodium thiocyanate) (**2**). Compound **1** (1.0 g, 3.87 mmol) and 0.314 g (3.87 mmol) of NaSCN were stirred in 1 ml of MeCN overnight, then heated and filtered. The clear soln. was allowed to cool overnight to r.t. whereupon slowly growing crystals began to form. After repeated washings with cold MeCN (*ca.* –40°), the crystals of **2** were dried under high vacuum to yield clear, slightly hygroscopic crystals. M.p. 141.0–142.0°. IR (KBr): 3700–3200*w*, 2980*m*, 2940*w*, 2050*s*, 2040*s*, 2038*s*, 1740*s*, 1730*s*, 1690*m*, 1450*m*, 1430*m*, 1385*s*, 1375*s*, 1310*s*, 1265*m*, 1190*s*, 1135*s*, 1110*m*, 1050*m*, 980*m*. Anal. calc. for $C_{51}H_{72}N_3Na_3O_{24}S_3$ (1276.31): C 47.99, H 5.69, N 3.29, S 7.54; found: C 47.98, H 5.85, N 3.20, S 7.43.

Bis[(4R,8R,12R)-4,8,12-trimethyl-1,5,9-trioxacyclododecane-2,6,10-trione] Bis(potassium thiocyanate) Monohydrate (**3**). Compound **1** (5.0, 19.4 mmol) and 1.88 (19.4 mmol) of KSCN were stirred in 5 ml of MeCN overnight, then filtered. The solvent was allowed to evaporate from the open flask, which allowed the uptake of sufficient amounts of H_2O from the atmosphere as well. Single crystals formed slowly; they were washed with cold MeCN (*ca.* –40°) and dried under high vacuum at r.t. M.p. 103.5–104.0°. IR (KBr): 3700–3100*m*, 2980*w*, 2940*w*, 2050*s*, 2040*s*, 1730*s*, 1725*s*, 1450*w*, 1420*w*, 1390*m*, 1380*m*, 1340*m*, 1310*s*, 1260*m*, 1240*w*, 1195*s*, 1190*s*, 1135*s*, 1110*m*, 1050*s*, 980*m*. Anal. calc. for $C_{26}H_{38}K_2N_2O_{13}S_2$ (728.92): C 42.84, H 5.25, N 3.84, S 8.80; found: C 42.87, H 5.36, N 3.72, S 7.97.

Bis[(4R,8R,12R)-4,8,12-trimethyl-1,5,9-trioxacyclododecane-2,6,10-trione] Bis(barium dithiocyanate) Dihydrate Monotetrahydrofurane Solvate (**4**). Compound **1** (1.0 g, 3.87 mmol) and 1.19 g (3.87 mmol) of $Ba(SCN)_2 \cdot 3\ H_2O$ were dissolved in 3 ml of THF and the solvent allowed to evaporate slowly, which led to the formation of crystals. The crystals were washed with cold THF (*ca.* –40°) and stored with some THF in the freezer. The crystals decomposed slowly in the laboratory atmosphere probably due to loss of coordinated THF. IR (KBr): 3700–3100*m*, 2980*w*, 2940*w*, 2040*s*, 1730*s*, 1720*s*, 1450*w*, 1420*w*, 1380*m*, 1310*s*, 1260*m*, 1195*s*, 1140*m*, 1115*m*, 1100*s*, 980*m*.

Crystal Structure Analysis of **3**: $C_{12}H_{18}O_6 \cdot KSCN \cdot 0.5\ H_2O$. The determination of the cell parameters and collection of the reflection intensities was performed on a *Picker-Stoe* four-circle diffractometer (graphite monochromatized MoK_α radiation, $\lambda = 0.7107$ Å); orthorhombic, space group $P2_12_12_1$ (No. 19), $a = 10.419$ (5), $b = 15.168$ (8), $c = 23.040$ (11) Å, $V = 3641$ (3) Å^3, $Z = 8$, $\rho_{calc.} = 1.33$ gcm^{-3}, $\mu = 0.43$ mm^{-1}, $F(000) = 1528$; $\omega/2\vartheta$-scan, $2.5 < 2\vartheta < 50°$, learnt-profile method; 3605 unique reflections, of which 2265 with $I > 2\sigma(I)$ were used for the solution (Direct Methods) and the refinement of the structure (SHELXTL-PLUS [31]). The non-H-atoms were refined anisotropically (unit weights), the H-atoms were added to this structure model with constant isotropic

temp. factors on calculated positions and refined using the riding model. The refinement converged finally at $R = 0.032$ (number of variables 406).

Crystal Structure Analysis of **4**: $C_{12}H_{18}O_6 \cdot Ba(SCN)_2 \cdot H_2O \cdot 0.5\ C_4H_8O$. The determination of the cell parameters and collection of the reflection intensities was performed on an *Enraf-Nonius CAD4* four-circle diffractometer (graphite monochromatized MoK_α radiation, $\lambda = 0.7107$ Å) at 173 K; trigonal, space group $P32$ (No. 145), $a = b = 12.598\ (5)$, $c = 25.071\ (10)$ Å, $V = 3446\ (4)$ Å^3, $Z = 6$, $\rho_{calc.} = 1.64$ gcm^{-3}, $\mu = 1.95$ mm^{-1}, $F(000) = 1692$; ω-scan, $0 < 2\vartheta < 50°$; the structure was solved by the *Patterson* method and refined by full-matrix least-squares (SHELXTL-PLUS [31]), using an exponentially modified weight factor with $r = 5$ Å^2 (heavy atoms anisotropic, except one triolide methylene C- and one H_2O O-atom, which were refined isotropically; H-atoms not included). The accuracy of the atomic parameters is reduced, because the crystal specimen was slightly twinned. The final refinement, based on 3250 reflections ($I > 3\sigma(I)$), converged to $R = 0.062$ ($R_w = 0.070$, number of variables 505).

Computational Details. H_{ii} parameters and *Slater* coefficients for H, C, N, O, S, and Na were the standard ones of the program EHMACC [24]. The ELF procedure was incorporated in the EHMACC program [25]. For the charge iteration, the valence orbital ionisation potentials were fitted to a quadratic equation. Parameters are taken from [32].

The three-dimensional (3D) color graphic representations of *Figs. 1, d*; *4, a–d*; and *9, a, b* were done using the color graphics package COLTURE [33], installed on *Silicon Graphics Indigo*^{2} and *IRIS 4D/320*, respectively, under the *Inventor* subsystem. The other 3D colour images in *Figs. 6, b*; *7, c, d*; and *8, a*, were obtained using the program package RAPTURE [34], installed on *IBM RS 6000* (3D graphic adapter GT4) and *Raster Technologies* work stations, respectively. The 2D pictures in *Figs. 6, a*; *7, a, b*; and *8, b–e*, were done by using the program GRAPA [35], installed on *Silicon Graphics* work stations.

REFERENCES

[1] D. Seebach, H.-M. Müller, H. M. Bürger, D. A. Plattner, *Angew. Chem.* **1992,** *104,* 443; *ibid. Int. Ed.* **1992,** *31,* 435 (preliminary communication).

[2] D. A. Plattner, A. Brunner, M. Dobler, H.-M. Müller, W. Petter, P. Zbinden, D. Seebach, *Helv. Chim. Acta* **1993,** *76,* 2004.

[3] Handbook of Chemistry and Physics, CRC Press, 60th edn.

[4] H.-M. Müller, D. Seebach, *Angew. Chem.* **1993,** *105,* 483; *ibid. Int. Ed.* **1993,** *32,* 477.

[5] R. N. Reusch, *Proc. Soc. Exp. Biol. Med.* **1989,** *191,* 377; R. N. Reusch, H. L. Sadoff, *Proc. Natl. Acad. Sci. U.S.A.* **1988,** *85,* 4176; R. N. Reusch, *FEMS Microbiol. Rev.* **1992,** *103,* 119.

[6] H. M. Bürger, D. Seebach, *Helv. Chim. Acta* **1993,** *76,* 2570.

[7] H.-M. Müller, Dissertation 9685, ETH-Zürich, 1992.

[8] G. Shoham, W. N. Lipscomb, U. Olsher, *J. Chem. Soc., Chem. Commun.* **1983,** 208; N. S. Poonia, A. V. Bajaj, *Chem. Rev.* **1979,** *79,* 389.

[9] D. Seebach, in 'Proceedings of the Robert A. Welch Foundation Conferences on Chemical Research. XXVII. Stereospecificity in Chemistry and Biochemistry, Nov. 7–9, 1983', Houston, Texas, 1984, p. 93; Ch. Schade, P. von Ragué Schleyer, *Adv. Organomet. Chem.* **1987,** *27,* 169; D. Seebach, *Angew. Chem.* **1988,** *100,* 1685; *ibid. Int. Ed.* **1988,** *27,* 1624; G. Boche, *Angew. Chem.* **1989,** *101,* 286; *ibid. Int. Ed.* **1989,** *28,* 277; K. Gregory, P. von Ragué Schleyer, R. Snaith, *Adv. Anorg. Chem.* **1991,** *37,* 47; P. G. Williard, in 'Comprehensive Organic Synthesis', Eds. B. M. Trost, I. Fleming, and S. L. Schreiber, Pergamon Press, Oxford, 1991, Vol. 1, p. 1–47; D. B. Collum, *Acc. Chem. Res.* **1993,** *26,* 227.

[10] M. Dobler, 'Ionophores and Their Structures', Wiley & Sons, New York, 1981; B. Dietrich, P. Viout, J.-M. Lehn, 'Macrocyclic Chemistry', VCH, Weinheim, 1993.

[11] a) T. B. Karpishin, T. M. Dewey, K. N. Raymond, *J. Am. Chem. Soc.* **1993,** *115,* 1842; T. B. Karpishin, K. N. Raymond, *Angew. Chem.* **1992,** *104,* 486; *ibid. Int. Ed.* **1992,** *31,* 466; b) M. J. Miller, F. Malouin, *Acc. Chem. Res.* **1993,** *26,* 241.

[12] R. Amstutz, J. D. Dunitz, T. Laube, W. B. Schweizer, D. Seebach, *Chem. Ber.* **1986,** *119,* 434.

[13] a) S. Shambayati, W. E. Crowe, S. L. Schreiber, *Angew. Chem.* **1990,** *102,* 273; *ibid. Int. Ed.* **1990,** *29,* 256; b) V. Sharma, M. Simard, J. D. Wuest, *J. Am. Chem. Soc.* **1992,** *114,* 7931, or M. Simard, J. Vaugeois, J. D. Wuest, *ibid.* **1993,** *115,* 370; c) S. E. Denmark, N. G. Almstead, *ibid.* **1993,** *115,* 3133.

[14] A. D. Becke, E. Edgecombe, *J. Chem. Phys.* **1990,** *92,* 5397.

[15] A. Savin, A. D. Becke, J. Flad, R. Nesper, H. G. von Schnering, *Angew. Chem.* **1991,** *103,* 421; *ibid. Int. Ed.* **1991,** *30,* 409.

[16] G.N. Lewis, *J. Am. Chem. Soc.* **1916,** *38,* 762; G.N. Lewis, 'Valence and the Structure of Atoms and Molecules', Chemical Catalog Co., New York, 1923.
[17] L. Pauling, *J. Am. Chem. Soc.* **1931,** *53,* 1367; J.C. Slater, *Phys. Rev.* **1931,** *37,* 481.
[18] E. Hückel, *Z. Physik* **1930,** *60,* 423; *ibid.* **1931,** *70,* 204.
[19] For an overview see: L. Pauling, 'The Nature of the Chemical Bond and the Structure of Molecules and Crystals', 3rd edn., Cornell University Press, Ithaka, 1960.
[20] R.B. Woodward, R. Hoffmann, 'The Conservation of Orbital Symmetry', Academic Press, New York, N.Y., 1969; K. Fukui, 'Theory of Orientation and Stereo Selection', Springer Verlag, Berlin, 1975.
[21] H. Weinstein, R. Pauncz, *Adv. Atom. Mol. Phys.* **1971,** *7,* 97; A. Reed, L. Curtiss, F. Weinhold, *Chem. Rev.* **1988,** *88,* 899.
[22] a) A. Savin, H.-J. Flad, J. Flad, H. Preuss, H.G. von Schnering, *Angew. Chem.* **1992,** *104,* 185; *ibid. Int. Ed.* **1992,** *31,* 185; b) A. Savin, O. Jepsen, J. Flad, O. Anderson, H. Preuss, H.G. von Schnering, *Angew. Chem.* **1992,** *104,* 186; *ibid. Int. Ed.* **1992,** *31,* 187; c) A. Burkhardt, U. Wedig, H.G. von Schnering, *Z. Anorg. Allg. Chem.* **1993,** *619,* 437.
[23] R. Hoffmann, W.N. Lipscomb, *J. Chem. Phys.* **1962,** *36,* 2179; *ibid.* **1962,** *37,* 2872; M.-H. Whangbo, R. Hoffmann, R.B. Woodward, *Proc. R. Soc. London [Ser.] A* **1979,** *366,* 23.
[24] The Extended Hückel program EHMACC was produced by M.-H. Whangbo, M. Evain, T. Hughbanks, M. Kertesz, S. Wijeyesekera, C. Wilker, C. Zheng, and R. Hoffmann.
[25] U. Häußermann, R. Nesper, ETH-Zürich 1993, unpublished.
[26] R. Gillespie, R.S. Nyholm, *Quat. Rev. Chem. Soc.* **1957,** *11,* 339; R. Gillespie, *J. Chem. Educ.* **1963,** *40,* 295; R. Gillespie, *Angew. Chem.* **1976,** *79,* 885; *ibid. Int. Ed.* **1976,** *6,* 819; R. Gillespie 'Molecular Geometry', Van Nostrand-Rheingold, London, 1972.
[27] T. Fässler, R. Nesper, unpublished results.
[28] M. Barrow, S. Cradock, E. Ebsworth, D. Rankin, *J. Chem. Soc., Dalton, Trans.* **1981,** 1988.
[29] W.B. Schweizer, J.D. Dunitz, *Helv. Chim. Acta* **1982,** *65,* 1547.
[30] P. Deslongchamps, 'Stereoelectronic Effects in Organic Chemistry', Pergamon Press, Oxford, 1983; A.J. Kirby, 'The Anomeric Effect and Related Stereoelectronic Effect of Oxygen', Springer-Verlag, Berlin, 1983.
[31] G.M. Sheldrick, SHELXTL-PLUS 88. Structure Determination Software Programs, Nicolet Instrument Corp., Madison, WI, 1988.
[32] H. Basch, A. Viste, H. Gray, *Theoret. Chim. Acta (Berlin)* **1965,** *3,* 458.
[33] P. Hofmann, R. Nesper, Program COLTURE, ETH-Zürich 1993, unpublished.
[34] R. Nesper, U. Wedig, B. Körner, H.G. von Schnering, Program RAPTURE, Max-Planck-Institut für Festkörperforschung, Stuttgart, 1989, unpublished.
[35] J. Flad, F.-X. Fraschio, B. Miehlich, Program GRAPA, Institut für Theoretische Chemie der Universität Stuttgart, 1989.